PNNL-24259

Pacific Northwest NATIONAL LABORATORY

Proudly Operated by Battelle Since 1965

Predictive Engineering Tools for Injection-Molded Long-Carbon-Fiber Thermoplastic Composites

Ba Nghiep Nguyen, Leonard S. Fifield
Pacific Northwest National Laboratory, Richland, WA 99352
Seth A. Kijewski, Michael D. Sangid
Purdue University, West Lafayette, IN 47907
Jin Wang, Franco Costa
Autodesk, Inc., Ithaca, NY 14850
Charles L. Tucker III
University of Illinois at Urbana-Champaign, Urbana, IL 61801
Raj N. Mathur
PlastiComp, Inc., Winona, MN 55987
Umesh N. Gandhi
Toyota Research Institute North America, Ann Arbor, MI 48105
Steven Mori
MAGNA Exteriors and Interiors Corporation, Aurora, Ontario, Canada

Project period: From October 1st 2012 to September 30th, 2016

Reporting period end date: March 31st, 2015
Quarterly report submitted to Aaron Yocum, National Energy Technology Laboratory, Morgantown, WV 26507

U.S. DEPARTMENT OF ENERGY

Prepared for the U.S. Department of Energy
under Contract DE-AC05-76RL01830

PNNL-24259

Predictive Engineering Tools for Injection-molded Long-Carbon-Fiber Thermoplastic Composites

Ba Nghiep Nguyen, Leonard S. Fifield
Pacific Northwest National Laboratory, Richland, WA 99352
Seth A. Kijewski, Michael D. Sangid
Purdue University, West Lafayette, IN 47907
Jin Wang, Franco Costa
Autodesk, Inc., Ithaca, NY 14850
Charles L. Tucker III
University of Illinois at Urbana-Champaign, Urbana, IL 61801
Raj N. Mathur
PlastiComp, Inc., Winona, MN 55987
Umesh N. Gandhi
Toyota Research Institute North America, Ann Arbor, MI 48105
Steven Mori
MAGNA Exteriors and Interiors Corporation, Aurora, Ontario, Canada

Project period: From October 1st 2012 to September 30th, 2016
Reporting period end date: March 31st, 2015

Quarterly report submitted to Aaron Yocum, National Energy Technology Laboratory, Morgantown, WV 26507

April 2015

Prepared for the U.S. Department of Energy under Contract DE-AC05-76RL01830, Pacific Northwest National Laboratory
Richland, Washington 99352

1. Objective

The objective of this project is to advance the *predictive engineering (PE) tool* to accurately predict *fiber orientation and length distributions* in *injection-molded long-carbon fiber thermoplastic composites* for optimum design of automotive structures using these materials *to meet weight and cost reduction requirements* defined in Table 2 of DE-FOA-0000648 (Area of Interest 1).

2. Background

This project proposes to integrate, optimize and validate the fiber orientation and length distribution models previously developed and implemented in the Autodesk Simulation Moldflow Insight (ASMI) package for injection-molded long-carbon-fiber thermoplastic composites. In our previous US Department of Energy (DOE) funded project, entitled "*Engineering Property Prediction Tools for Tailored Polymer Composite Structures,*" Pacific Northwest National Laboratory (PNNL), with the University of Illinois and Autodesk, Inc., developed a unique assembly of computational algorithms providing state-of-the-art process and constitutive models that enhance the capabilities of commercial software packages to predict fiber orientation and length distributions as well as subsequent mechanical properties of injection-molded long-fiber thermoplastic (LFT) composites. These predictive capabilities were validated using fiber analysis data generated at Oak Ridge National Laboratory on two-dimensional (2-D) structures of edge-gated plaques or center-gated disks injection-molded from long-glass-fiber/polypropylene (PP) or long-glass-fiber/polyamide 6,6 (PA66) pellets. The present effort aims at rendering the developed models more robust and efficient to automotive industry part design to achieve weight savings and cost reduction. This ultimate goal will be achieved by optimizing the developed models, improving and integrating their implementations in ASMI, and validating them for a complex three-dimensional (3D) long-carbon fiber (LCF) thermoplastic automotive part. Both PP and PA66 are used for the resin matrices. Local fiber orientation and length distributions at the key regions on the part are measured for the model validation based on a 15% accuracy criterion. The project outcome will be the ASMI package enhanced with computational capabilities to accurately predict fiber orientation and length distributions in automotive parts designed with long-carbon fiber thermoplastics.

3. Accomplishments

During the second quarter of FY 2015, the following technical progress has been made toward project milestones:

1) Autodesk reviewed 3D fiber orientation distribution (FOD) comparisons and provided support on improving accuracy.
2) Autodesk reviewed fiber length distribution (FLD) data comparisons and provided suggestions, assisted PNNL in FOD and FLD parameter settings optimization, and advised PNNL on appropriate through thickness thermal conductivity for improved frozen layer effect on FOD predictions. Autodesk also participated in project review meetings including preparations and discussions towards passing the go/no-go decision point.
3) Autodesk implemented an improved FOD inlet profile specification method through the part thickness for 3D meshes and provided an updated ASMI research version to PNNL.
4) The University of Illinois (Prof. C.L. Tucker) provided Autodesk with ideas to improve fiber orientation modeling.
5) Purdue University re-measured fiber orientation for the fast-fill 50wt% LCF/PA66 edge-gated plaque and delivered the fiber orientation data for this plaque at the selected locations (named A, B, and C, Figure 1) to PNNL. Purdue also re-measured fiber orientation for locations A on the fast-fill 30wt% LCF/PP and 50wt% LCF/PA66 center-gated plaques, which exhibited anomalous fiber orientation behavior.

6) Purdue University conducted fiber length measurements and delivered the length data to PNNL for the purge materials (slow-fill 30wt% LCF/PP and 30wt% LCF/PA66 purge materials) and plaques selected on the go/no-go list for fiber length model validation (i.e., slow-fill edge-gated 30wt% LCF/PP and 30wt% LCF/PA66 plaques, Locations A, B, and C).
7) PNNL developed a method to recover intact carbon fibers from LCF/PA66 materials. Isolated fibers were shipped to Purdue for length distribution analysis.
8) PNNL completed ASMI mid-plane analyses for all the plaques defined on the go/no-go list for fiber orientation (FO) model validation and compared the predicted fiber orientations with the measured data provided by Purdue at Locations A, B, and C on these plaques. The 15% accuracy criterion based on evaluation of tensile and bending stiffness was used to assess the accuracy in fiber orientation predictions.
9) PNNL completed ASMI mid-plane analyses for all the plaques defined on the go/no-go list for fiber length distribution (FLD) model validation and compared the predicted length distributions with the measured data provided by Purdue at Locations A, B, and C on these plaques. The 15% accuracy criterion based on evaluation of tensile and bending stiffness was used to assess the accuracy in fiber length predictions.
10) PNNL tested the new ASMI version received from Autodesk in March 2015, examined and discussed 3D fiber orientation predictions for PlastiComp plaques.
11) PlastiComp, Inc. (PlastiComp), Toyota Research Institute North America (Toyota) and Magna Exteriors and Interiors Corporation (Magna) participated in discussions with team members on the go/no-go plan. Toyota continued the discussion with Magna on tool modification for molding the complex part in order to achieve the target fiber length in the part.

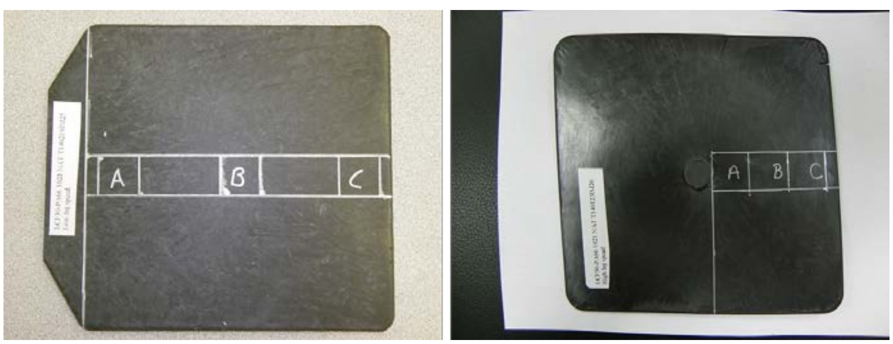

Figure 1. Locations A, B and C defined on the edge-gated (left) and center-gated (right) plaques where samples were removed for fiber orientation and length measurements.

4. Progress and Status

4.1 Fiber Orientation Predictions

PNNL received the re-measured data from Purdue for the fast-fill 50wt% LCF/PA66 edge-gated plaque on the go/no-go list and then conducted ASMI mid-plane injection molding analysis for this plaque to predict the resulting fiber orientation distribution using the anisotropic rotary diffusion reduced strain closure (ARD-RSC) model [1]. PNNL also completed the ASMI mid-plane analyses of all the PlastiComp plaques on the go/no-go list for the validation of ASMI fiber orientation modeling. The details of mid-plane and 3D ASMI analyses of the PlastiComp plaques adopted for the go/no-go list will be presented in a Topical Report that summarizing the entire project at project completion.

4.1.1 Mid-plane ASMI Fiber Orientation Predictions

Figures 2, 3 and 4 report the comparisons between the predicted and measured fiber orientation components in the flow and cross-flow directions (A_{11} and A_{22}) for Locations A, B and C on the fast-fill 50wt% LCF/PA66 edge-gated plaque. Tables 1 to 4 provide the tensile and flexural moduli calculated based on the predicted and measured fiber orientations for these locations. There is global agreement of results for Locations A and B and agreement on three moduli at Location C, while the tensile modulus E_{11} for Location C based on predicted fiber orientation significantly exceeds the computed value based on measured fiber orientation for this location. Figure 4 shows a significant asymmetry of the measured fiber orientation distributions about the plaque mid plane that cause larger deviations between moduli based on predicted and measured fiber orientations for Location C.

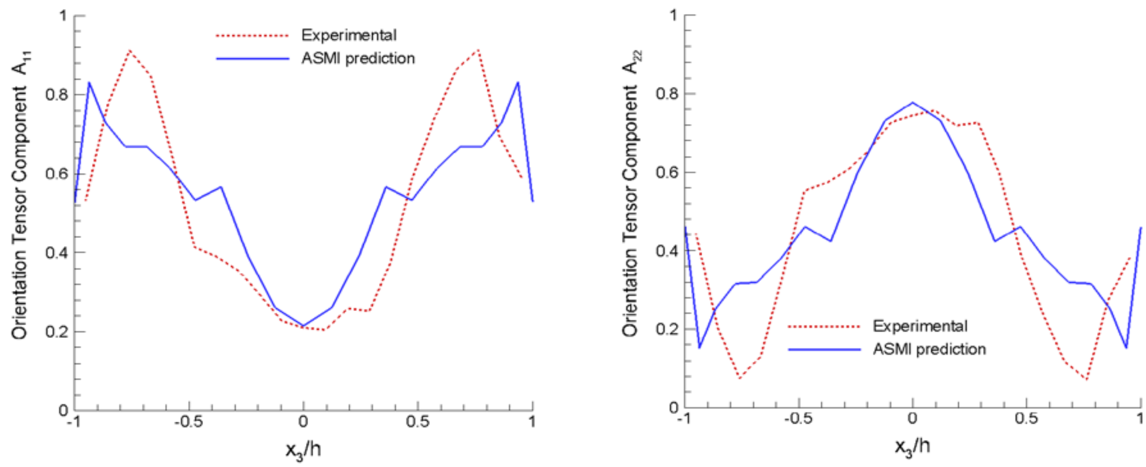

(a) (b)

Figure 2: Predictions vs. measured data for the fiber orientation tensor components: (a) A_{11}, and (b) A_{22} for Location A on the fast-fill 50wt% LCF/PA66 edge-gated plaque.

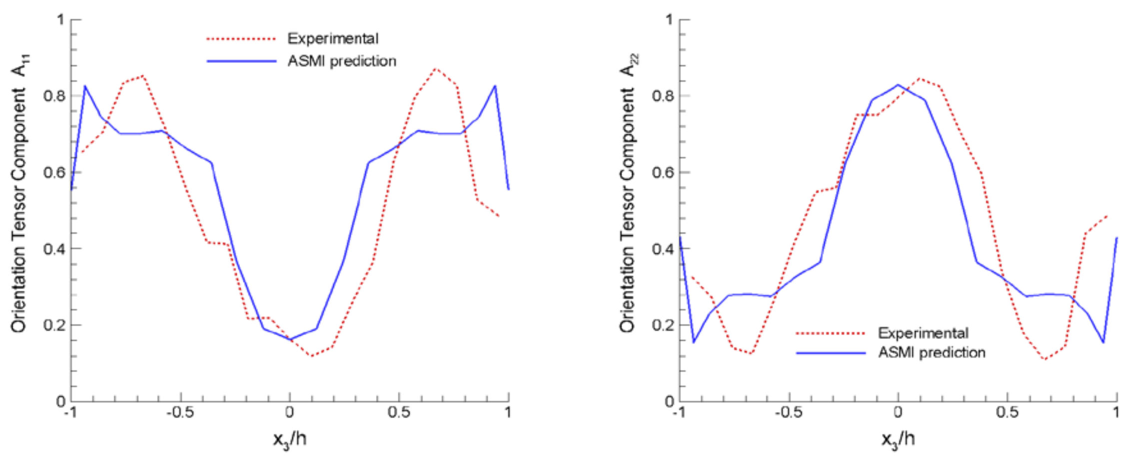

(a) (b)

Figure 3: Predictions vs. measured data for the fiber orientation tensor components: (a) A_{11}, and (b) A_{22} for Location B on the fast-fill 50wt% LCF/PA66 edge-gated plaque.

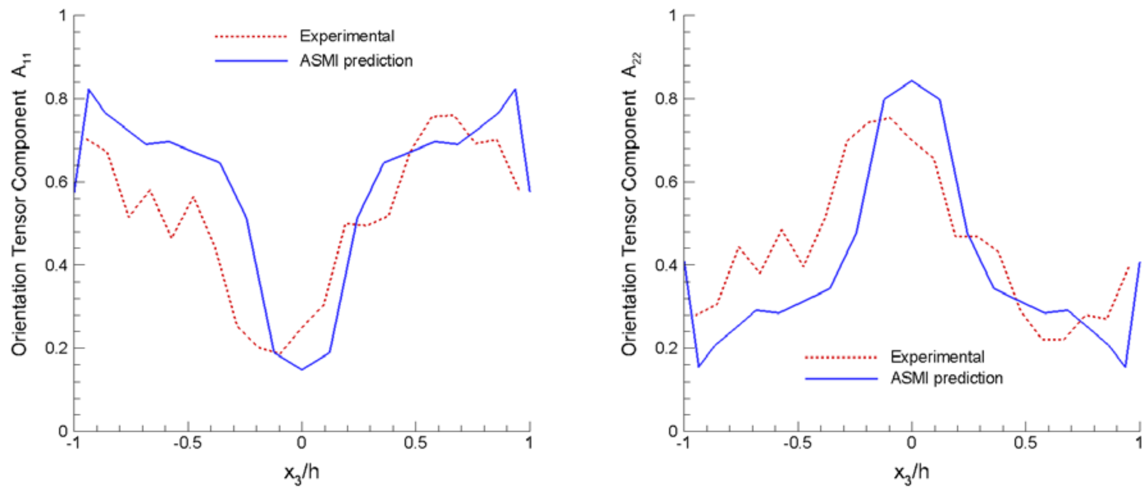

(a) (b)

Figure 4: Predictions vs. measured data for the fiber orientation tensor components: (a) A_{11}, and (b) A_{22} for Location C on the fast-fill 50wt% LCF/PA66 edge-gated plaque.

Tensile Modulus	E_{11} (predicted orientation) MPa	E_{11} (measured orientation) MPa	Agreement within
Loc. A	45943	44475	3.30%
Loc. B	49201	43492	13.13%
Loc. C	50990	41143	23.93%

Table 1. Computed E_{11} based on measured and predicted fiber orientations at Locations A, B and C in the fast-fill 50wt% LCF/PA66 edge-gated plaque.

Tensile Modulus	E_{22} (predicted orientation) MPa	E_{22} (measured orientation) MPa	Agreement within
Loc. A	34103	36867	7.50%
Loc. B	32375	38431	15.76%
Loc. C	30646	35210	12.96%

Table 2. Computed E_{22} based on measured and predicted fiber orientations at Locations A, B and C in the fast-fill 50wt% LCF/PA66 edge-gated plaque.

Flexural Modulus	D_{11} (predicted orientation) MPa.mm^3	D_{11} (measured orientation) MPa.mm^3	**Agreement within**
Loc. A	165658	174469	5.05%
Loc. B	173757	167242	3.90%
Loc. C	177420	155060	14.42%

Table 3. Computed D_{11} based on measured and predicted fiber orientations at Locations A, B and C in the fast-fill 50wt% LCF/PA66 edge-gated plaque.

Flexural Modulus	D_{22} (predicted orientation) MPa.mm^3	D_{22} (measured orientation) MPa.mm^3	**Agreement within**
Loc. A	79205	73384	7.93%
Loc. B	71851	77518	7.31%
Loc. C	68483	81897	16.38%

Table 4. Computed D_{22} based on measured and predicted fiber orientations at Locations A, B and C in the fast-fill 50wt% LCF/PA66 edge-gated plaque.

4.1.2 3D ASMI Fiber Orientation Predictions

PNNL recently received a new version of ASMI from Autodesk that incorporates improvements in 3D prediction of fiber orientation. In this version, a new option was added to apply the prescribed inlet orientation profile through the thickness direction of the part around the gate. PNNL has tested the new version and preliminary results are presented in this report. Figures 5a and 5b show the 3D finite element meshes that were used in the 3D ASMI analyses of PlastiComp plaques to predict fiber orientations in these plaques.

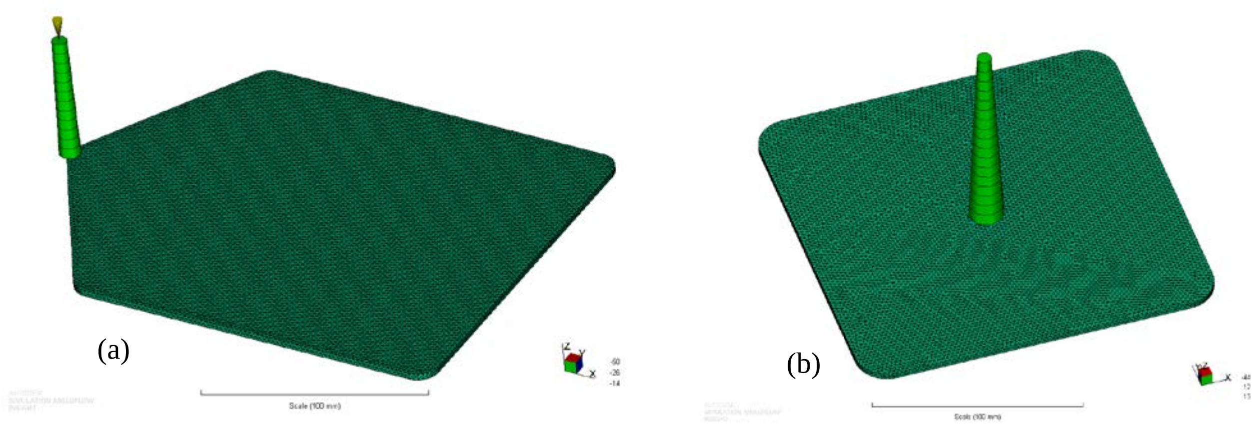

Figure 5. 3D ASMI models for (a) edge-gated plaque, and (b) center-gated plaque.

Figures 6 to 8 show the 3D fiber orientation predictions for A_{11} and A_{22} for Locations A, B and C on the slow-fill 50wt% LCF/PP edge-gated plaque. These figures also report the mid-plane analysis results previously obtained and the measured fiber orientation data received from Purdue. There is good agreement of results observed for Location A where both 3D and mid-plane solutions have reasonable agreement with the experimental data. The 3D model predicts a similar wide core as predicted in the mid-plane results, but it underestimated A_{11} and overestimated A_{22} in the shell layers. This was also observed for Location B on the same plaque. However, the 3D results for Location C are in better agreement with the average measured data than with the mid-plane solution (Figure 8).

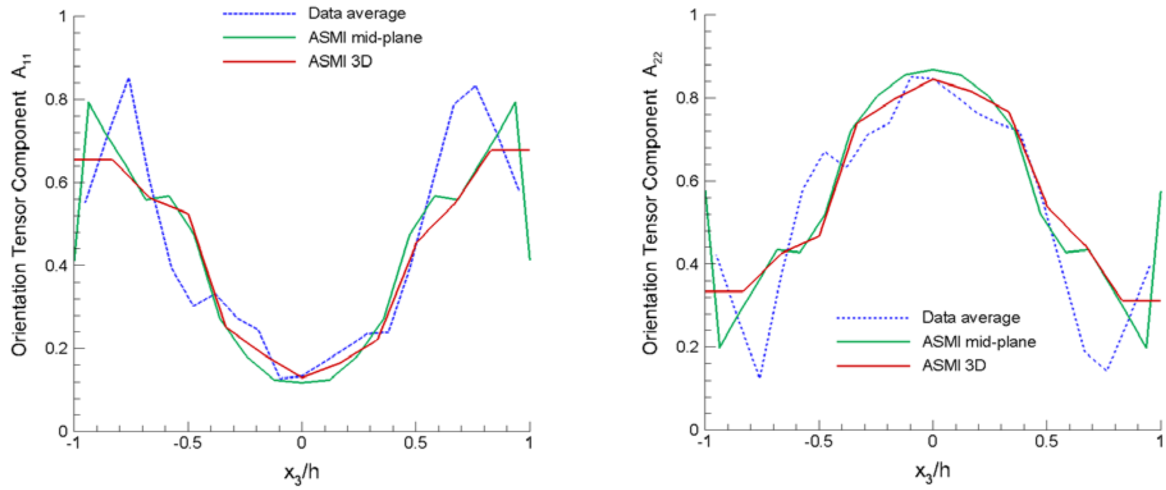

(a) (b)

Figure 6: Predictions vs. measured data for the fiber orientation tensor components: (a) A_{11}, and (b) A_{22} for Location A on the slow-fill 50wt% LCF/PP edge-gated plaque.

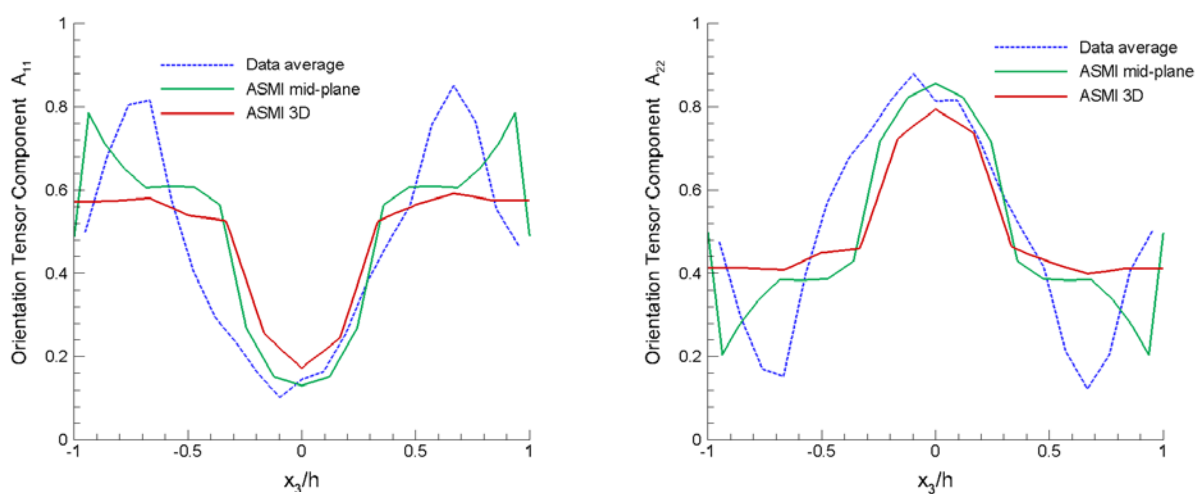

(a) (b)

Figure 7: Predictions vs. measured data for the fiber orientation tensor components: (a) A_{11}, and (b) A_{22} for Location B on the slow-fill 50wt% LCF/PP edge-gated plaque.

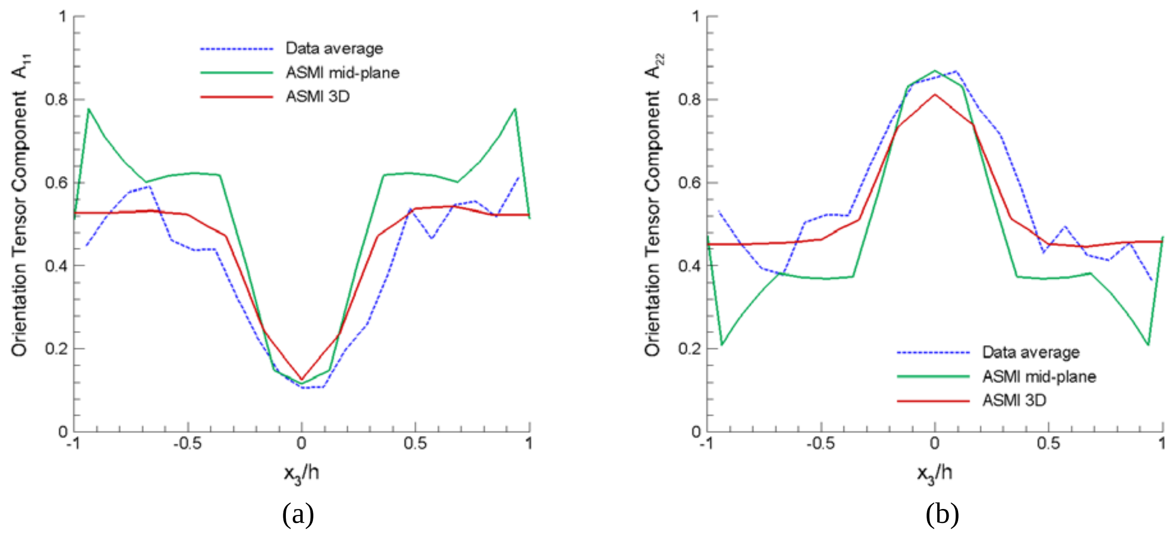

Figure 8: Predictions vs. measured data for the fiber orientation tensor components: (a) A_{11}, and (b) A_{22} for Location C on the slow-fill 50wt% LCF/PP edge-gated plaque.

Tables 5 to 8 report the tensile and flexural moduli calculated based on the predicted and measured fiber orientations for Locations A, B and C on this plaque. These tables compare both mid-plane and 3D moduli results with the corresponding values computed using measured fiber orientation data. The percentages within which the predictions agree with the data are also provided in these tables. The mid-plane results agree with the measured data within 15% except for the predictions for Location C that do not meet the 15% accuracy criterion. As earlier mentioned, Figure 8 shows that the predicted mid-plane A_{11} for Location C is above the experimental curve while the predicted mid-plane A_{22} is below the experimental one, this has resulted in significant differences in the values of computed moduli for this location. The results reported in Tables 5 to 8 show that 3D predictions agree well with the measured data (within 15%) for all three locations examined.

Tensile Modulus	E_{11} (mid-plane orientation) MPa	E_{11} (3D orientation) MPa	E_{11} (measured orientation) MPa
Loc. A	30371 (4.79%)	29077 (0.32%)	28984
Loc. B	34736 (10.54%)	30257 (3.72%)	31425
Loc. C	35965 (45.77%)	26596 (7.80%)	24672

Table 5. Computed E_{11} based on measured and predicted fiber orientations at Locations A, B and C in the slow-fill 50wt% LCF/PP edge-gated plaque.

Tensile Modulus	E_{22} (mid-plane orientation) MPa	E_{22} (3D orientation) MPa	E_{22} (measured orientation) MPa
Loc. A	36083 (0.19%)	36054 (0.27%)	36153
Loc. B	30179 (10.46%)	31599 (6.25%)	33704
Loc. C	28394 (23.46%)	34481 (7.05%)	37095

Table 6. Computed E_{22} based on measured and predicted fiber orientations at Locations A, B and C in the slow-fill 50wt% LCF/PP edge-gated plaque.

Flexural Modulus	D_{11} (mid-plane orientation) MPa.mm^3	D_{11} (3D orientation) MPa.mm^3	D_{11} (measured orientation) MPa.mm^3
Loc. A	121362 (4.26%)	120868 (4.65%)	126761
Loc. B	129217 (3.18%)	109921 (12.23%)	125239
Loc. C	130646 (30.26%)	98981 (1.32%)	100300

Table 7. Computed D_{11} based on measured and predicted fiber orientations at Locations A, B and C in the slow-fill 50wt% LCF/PP edge-gated plaque.

Flexural Modulus	D_{22} (mid-plane orientation) MPa.mm^3	D_{22} (3D orientation) MPa.mm^3	D_{22} (measured orientation) MPa.mm^3
Loc. A	78584 (10.80%)	71648 (1.02%)	70924
Loc. B	69276 (2.09%)	78376 (10.77%)	70755
Loc. C	66765 (24.17%)	86960 (1.24%)	88048

Table 8. Computed D_{22} based on measured and predicted fiber orientations at Locations A, B and C in the slow-fill 50wt% LCF/PP edge-gated plaque.

Figures 9 to 11 show the 3D fiber orientation predictions for A_{11} and A_{22} for Locations A, B and C on the slow-fill 50wt% LCF/PP center-gated plaque. These figures also report the mid-plane analysis results previously obtained and the measured orientation data received from Purdue. Due to a significant missaligment between the flow direction and the measurement surface at Location A, the orientation data received for this location were corrected by the method presented in our previous report [2]. The mid-plane model very well captured the corrected fiber orientation data at Location A while the 3D model underpredicted A_{11} and overpredicted A_{22}. Both mid-plane and 3D results correlate quite well with the measured data for Location B. A significant asymmetry in measured fiber orientation about the plaque mid plane has been observed for Location C, and this asymmetry could not be captured by either model.

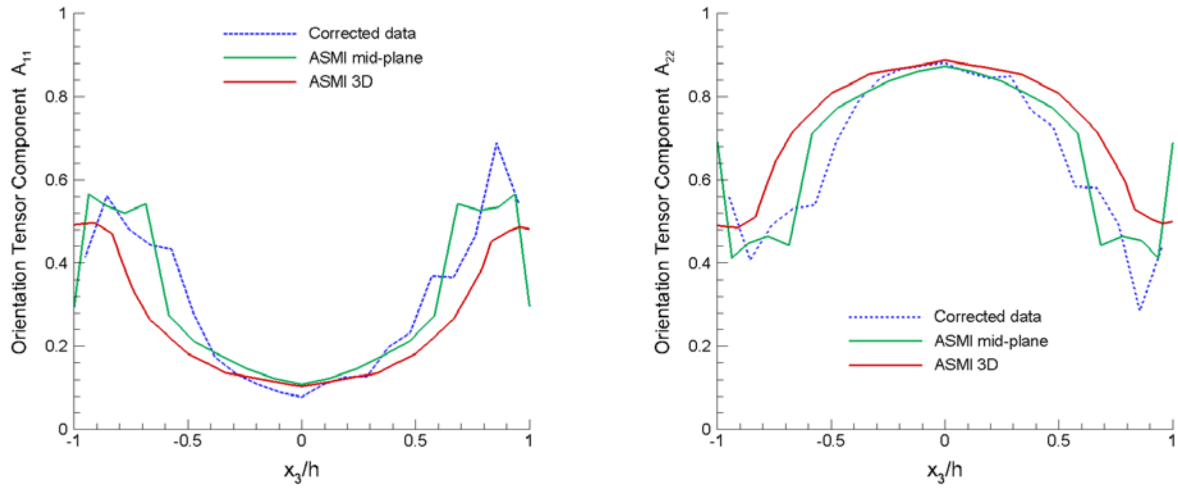

(a) (b)

Figure 9: Predictions vs. measured data for the fiber orientation tensor components: (a) A_{11}, and (b) A_{22} for Location A on the slow-fill 50wt% LCF/PP center-gated plaque.

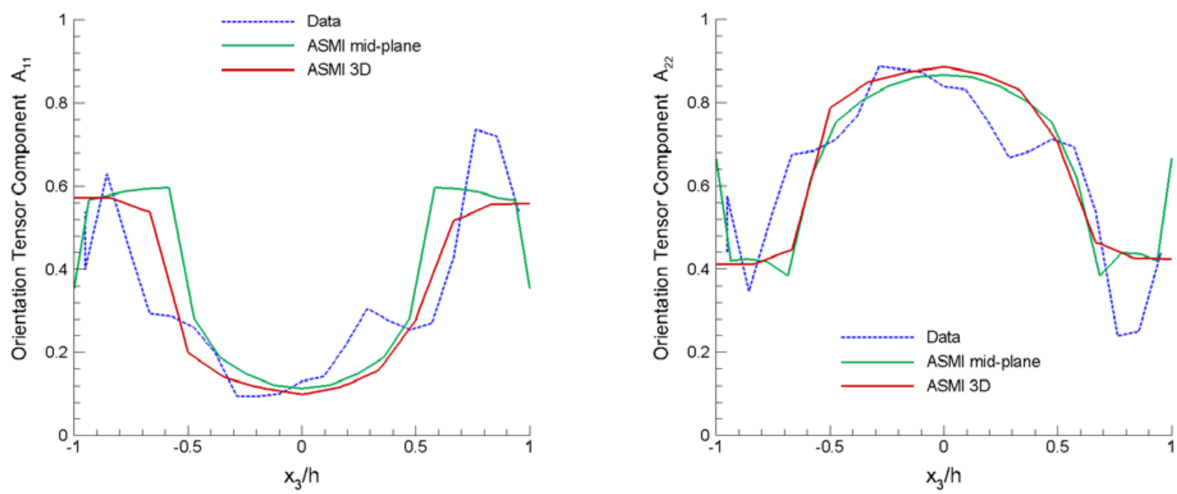

(a) (b)

Figure 10: Predictions vs. measured data for the fiber orientation tensor components: (a) A_{11}, and (b) A_{22} for Location B on the slow-fill 50wt% LCF/PP center-gated plaque.

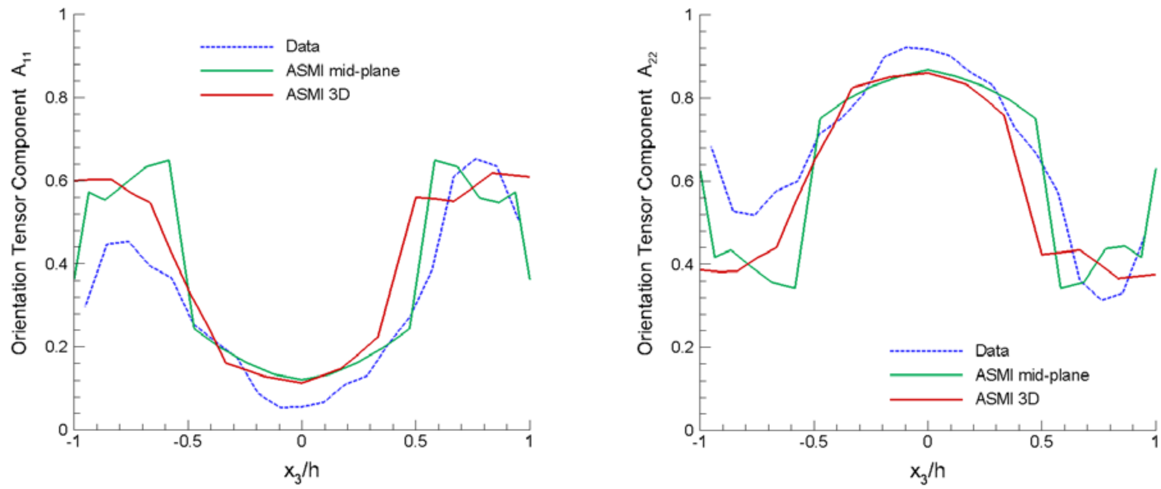

(a) (b)

Figure 11: Predictions vs. measured data for the fiber orientation tensor components: (a) A_{11}, and (b) A_{22} for Location C on the slow-fill 50wt% LCF/PP center-gated plaque.

Tables 9 to 12 exhibit the tensile and flexural moduli calculated based on predicted and measured fiber orientations for Locations A, B and C of the plaque. These tables compare both mid-plane and 3D results with the corresponding moduli computed using measured fiber orientation data. The mid-plane results agree with the measured data within 15% except for the prediction for E_{11} at Location C that exceeds 15% due to the high asymmetry of the measured fiber orientation data at this location. The 3D model underpredicted A_{11} and overpredicted A_{22} at Location A resulting in significantly lower E_{11} and D_{11} but significantly higher E_{22} and D_{22} compared to the values computed using measured orientation data for this location. However, this model overpredicted A_{11} and underpredicted A_{22} at Location C leading to significantly higher E_{11} and D_{11} but significantly lower E_{22} and D_{22} compared to the values computed using measured orientation data for this location.

Tensile Modulus	$\boldsymbol{E_{11}}$ (mid-plane orientation) MPa	$\boldsymbol{E_{11}}$ (3D orientation) MPa	$\boldsymbol{E_{11}}$ (measured orientation) MPa
Loc. A	20634 (8.20%)	15780 (17.26%)	19071
Loc. B	23064 (13.49%)	19767 (2.73%)	20322
Loc. C	24895 (31.52%)	25386 (34.12%)	18928

Table 9. Computed E_{11} based on measured and predicted fiber orientations at Locations A, B and C in the slow-fill 50wt% LCF/PP center-gated plaque.

Tensile Modulus	E_{22} (mid-plane orientation) MPa	E_{22} (3D orientation) MPa	E_{22} (measured orientation) MPa
Loc. A	46206 (0.66%)	52307 (13.95%)	45905
Loc. B	43152 (3.60%)	47654 (6.46%)	44762
Loc. C	41155 (11.37%)	39216 (15.54%)	46432

Table 10. Computed E_{22} based on measured and predicted fiber orientations at Locations A, B and C in the slow-fill 50wt% LCF/PP center-gated plaque.

Flexural Modulus	D_{11} (mid-plane orientation) MPa.mm^3	D_{11} (3D orientation) MPa.mm^3	D_{11} (measured orientation) MPa.mm^3
Loc. A	86552 (1.92%)	71394 (19.09%)	88242
Loc. B	93178 (0.36%)	91294 (1.28%)	92847
Loc. C	97653 (14.04%)	107745 (25.82%)	85631

Table 11. Computed D_{11} based on measured and predicted fiber orientations at Locations A, B and C in the slow-fill 50wt% LCF/PP center-gated plaque.

Flexural Modulus	D_{22} (mid-plane orientation) MPa.mm^3	D_{22} (3D orientation) MPa.mm^3	D_{22} (measured orientation) MPa.mm^3
Loc. A	110144 (7.57%)	120184 (17.38%)	102389
Loc. B	101783 (0.85%)	98817 (2.09%)	100929
Loc. C	96389 (8.71%)	81032 (23.26%)	105591

Table 12. Computed D_{22} based on measured and predicted fiber orientations at Locations A, B and C in the slow-fill 50wt% LCF/PP center-gated plaque.

4.2 Fiber Length Prediction

The reduced order length model (ROM) using proper orthogonal decomposition (POD) [3-4] was implemented in ASMI by Autodesk. Autodesk delivered to PNNL a research version of ASMI containing this model. PNNL conducted ASMI analyses for the PlastiComp plaques adopted on the go/no-go list for validation of the fiber length model. The plaques considered were the slow-fill 30wt% LCF/PP and slow-fill 30wt% CF/PA66 edge-gated plaques. With PNNL's assistance in separation and recovery of fibers, Purdue performed fiber length measurements for these plaques at Locations A, B, and C and delivered the length data to PNNL. As the use of the fiber length model requires the length data in the feeding system introduced as the inlet condition, Purdue also performed fiber length measurements on fibers isolated from 30 wt%CF/PP by Purdue and from 30wt%CF/PA66 by PNNL from the corresponding purge materials taken from the injection molding nozzles. Figures 12a and 12b show the fiber length distributions in the nozzles for the above-mentioned moldings. The corresponding weight-average lengths L_w are also provided in these figures.

The fiber length attrition model [3] contains 3 parameters that needs to be identified through numerical simulations. These parameters are the anisotropic drag coefficient, D_g that governs fiber breakage, the shear rate constant, C_b that scales the breakage rate, and the probability profile control factor, S that controls the profile of the length distribution. Using the nozzle length data applied as fiber inlet condition at the injection location, a series of ASMI injection molding simulations were conducted for the slow-fill 30wt% LCF/PP and slow-fill 30wt% CF/PA66 edge-gated plaques to identify these parameters to produce good correlations between predicted and measured FLDs at Locations A, B, and C. The accuracy in fiber length prediction was determined using the 15% accuracy criterion that was evaluated via the principal tensile and flexural moduli computed using predicted vs. measured FLDs for a prescribed fiber orientation distribution. In this work, predicted fiber orientations were used in the computation of moduli. Fiber length analyses were performed with 10 POD modes using midplane models.

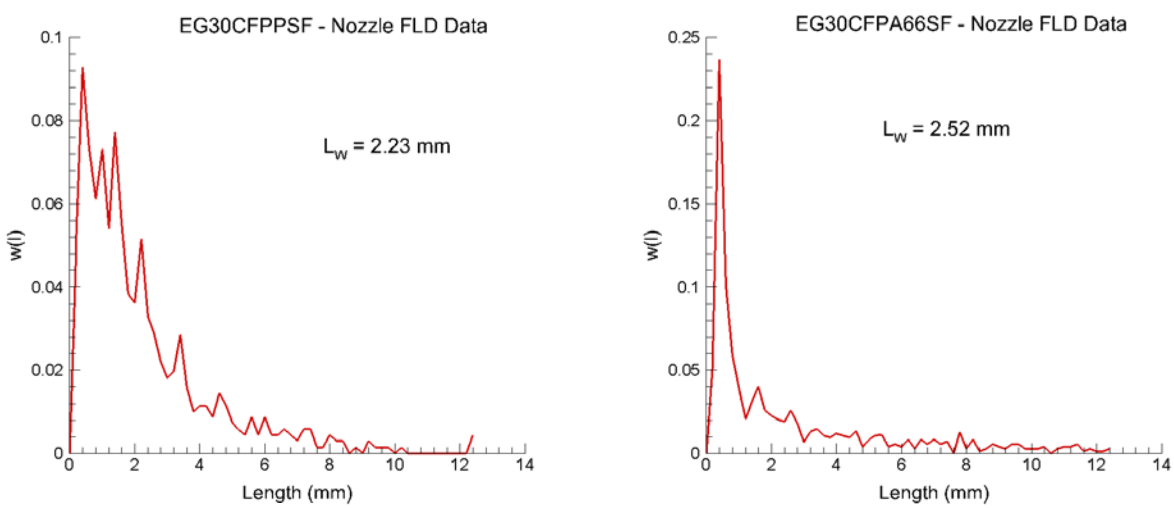

(a) (b)

Figure 12. Measured fiber length distributions of: (a) slow-fill 30wt% LCF/PP and (b) slow-fill 30wt% CF/PA66 purge materials.

Figures 13 to 15 respectively report the predicted FLDs compared to measured FLDs for Locations A, B and C on the slow-fill 30wt% LCF/PP plaque. The weight-average lengths resulting from the predicted and measured distributions are also given in these figures. The fiber length model is able to capture the measured length distributions quite well. Also, there is a reasonable agreement in weight-average lengths.

Tables 13 to 16 provide the tensile and flexural moduli calculated based on the predicted and measured FLDs for Locations A, B and C on the slow-fill 30wt% LCF/PP plaque. Very good agreement of results are observed for all three locations. The excellent agreement in predicted stiffness performance is not surprising since the fiber length distributions achieved represent truly long fibers producing high fiber aspect ratio values that bring the elastic moduli near their maximum limits. Changes in fiber length in this high aspect ratio range have only very little effect on the composite elastic moduli. The saturation of elastic moduli with fiber length and aspect ratio is illustrated in Figures 16a and 16b for the tensile modulus E_{11} and flexural modulus D_{11} for the 30wt% LCF/PP material. This sensitivity analysis for fiber length was performed by considering fiber lengths from very short fibers to very long fibers approaching continuous fibers while computing the tensile and flexural moduli using the predicted fiber orientation at Location B on this plaque. The results reported in Figures 16a and 16b clearly show that the moduli are close to their limits for lengths greater than 1 mm. For example, for a length of 1.4 mm corresponding to the fiber aspect ratio of 200 the moduli are within 2.5% of their respective limits. The weight average lengths at Locations A, B, and C on this plaque are in the 2-mm range which represents very long fibers.

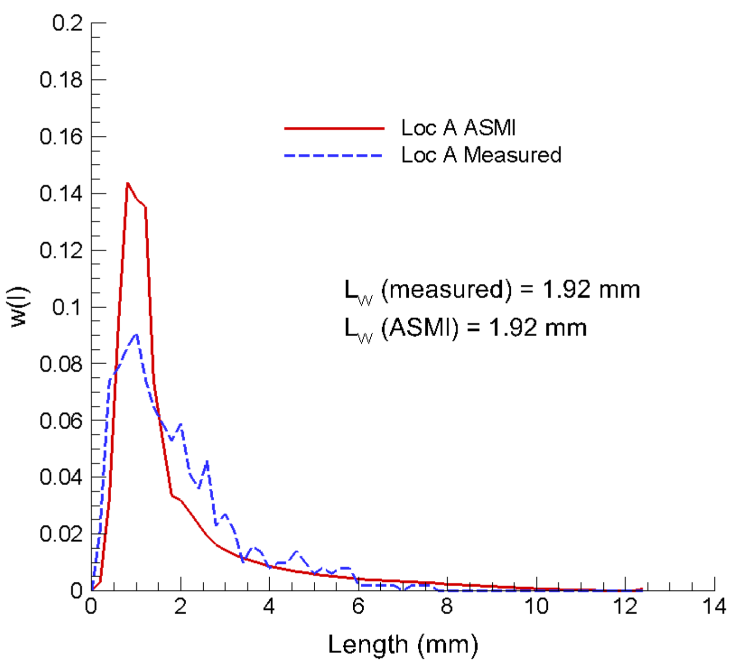

Figure 13. Predicted and measured fiber length distributions for Location A on the slow-fill 30wt% LCF/PP plaque.

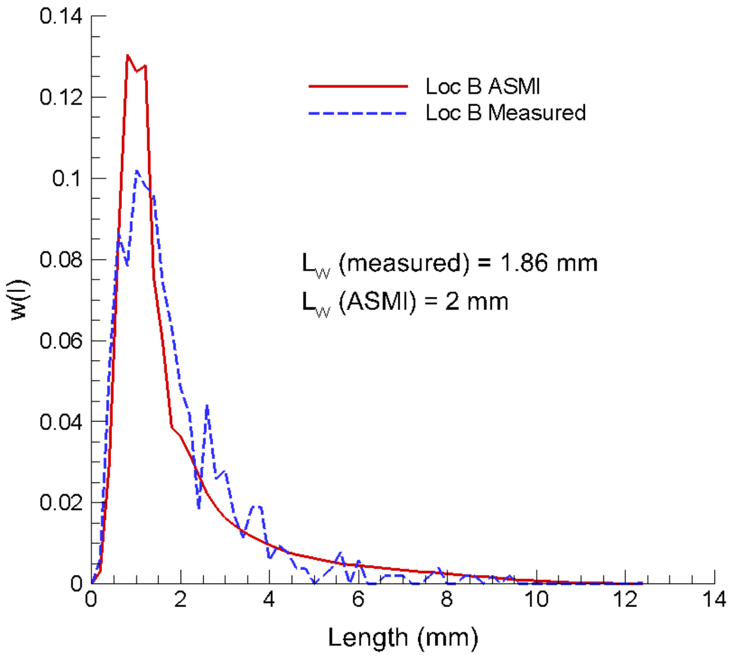

Figure 14. Predicted and measured fiber length distributions for Location B on the slow-fill 30wt% LCF/PP plaque.

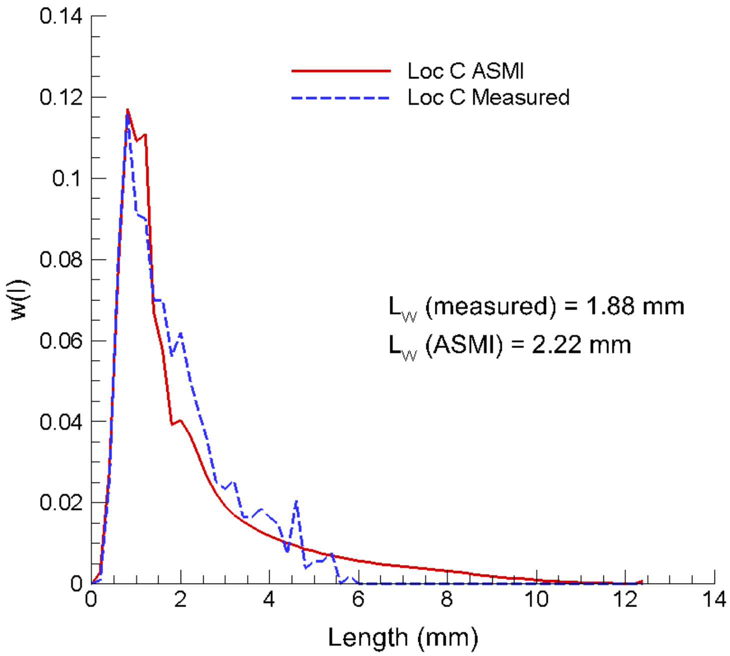

Figure 15. Predicted and measured fiber length distributions for Location C on the slow-fill 30wt% LCF/PP plaque.

Tensile Modulus	E_{11} (predicted FLD) MPa	E_{11} (measured FLD) MPa	Agreement within
Loc. A	14978	14860	0.79%
Loc. B	13053	13027	0.20%
Loc. C	12594	12612	0.14%

Table 13. Computed E_{11} based on measured and predicted fiber length distributions at Locations A, B and C in the slow-fill 30wt% LCF/PP edge-gated plaque.

Tensile Modulus	E_{22} (predicted FLD) MPa	E_{22} (measured FLD) MPa	Agreement within
Loc. A	17990	17843	0.82%
Loc. B	19419	19378	0.21%
Loc. C	18605	18633	0.15%

Table 14. Computed E_{22} based on measured and predicted fiber length distributions at Locations A, B and C in the slow-fill 30wt% LCF/PP edge-gated plaque.

Flexural Modulus	D_{11} (predicted FLD) $MPa.mm^3$	D_{11} (measured FLD) $MPa.mm^3$	Agreement within
Loc. A	59243	58802	0.75%
Loc. B	54131	54030	0.19%
Loc. C	51291	51360	0.13%

Table 15. Computed D_{11} based on measured and predicted fiber length distributions at Locations A, B and C in the slow-fill 30wt% LCF/PP edge-gated plaque.

Flexural Modulus	D_{22} (predicted FLD) MPa.mm^3	D_{22} (measured FLD) MPa.mm^3	**Agreement within**
Loc. A	45378	45067	0.69%
Loc. B	46184	46102	0.18%
Loc. C	44323	44379	0.13%

Table 16. Computed D_{22} based on measured and predicted fiber length distributions at Locations A, B and C in the slow-fill 30wt% LCF/PP edge-gated plaque.

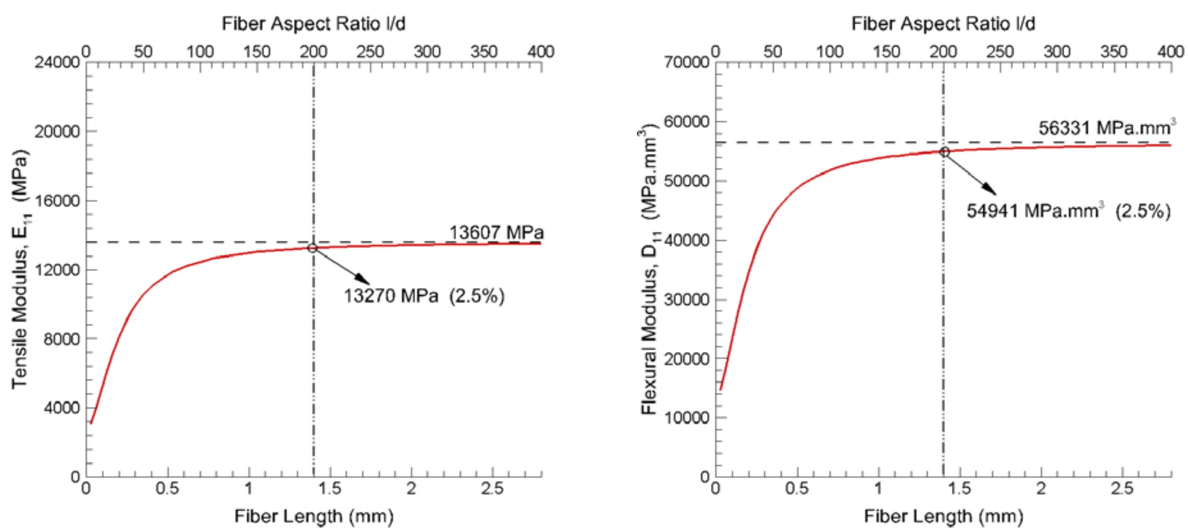

(a) (b)

Figure 16. Sensitivity analysis of fiber length showing saturation of elastic moduli in the range of long fibers for the 30wt% LCF/PP molding – (a) E_{11} and (b) D_{11}.

A similar ASMI analysis was performed for the slow-fill 30wt% LCF/PA66 plaque to predict FLDs at Locations A, B and C on this plaque for the validation of the fiber length model. Figures 17 to 19, respectively, report the predicted FLDs compared to measured FLDs for these locations. The weight-average lengths resulting from the predicted and measured distributions are also given in the same figures. As observed in the LCF/PP molding discussed above, the fiber length model was also able to capture the measured length distributions in the LCF/PA66 molding quite well. Also, there is a reasonable agreement in weight-average lengths. Tables 17 to 20 provide the tensile and flexural moduli calculated based on the predicted and measured FLDs for all three locations on this plaque. Very good agreements of results are observed for all three locations. A sensitivity analysis for fiber length was again conducted and demonstrated that truly long fibers were also achieved in this molding where the tensile and flexural moduli are close to their achievable limits (Figure 20).

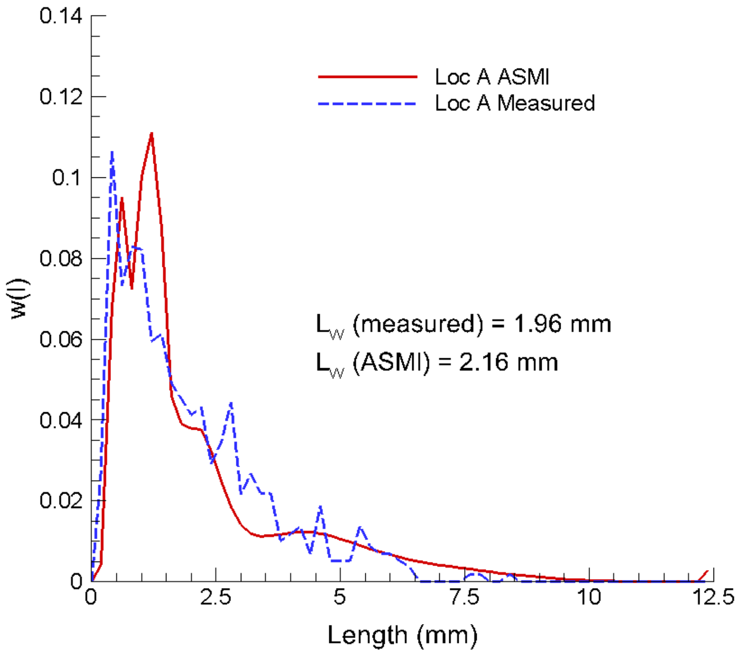

Figure 17. Predicted and measured fiber length distributions for Location A on the slow-fill 30wt% LCF/PA66 plaque.

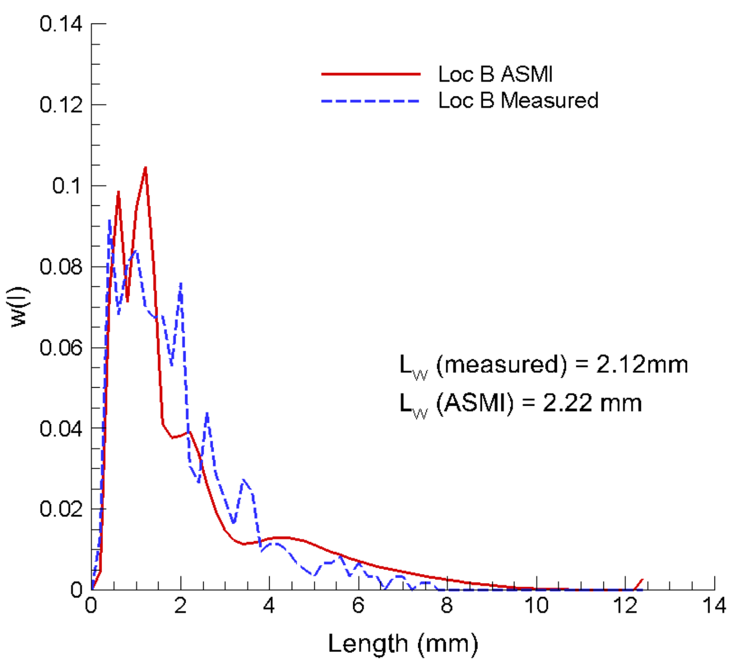

Figure 18. Predicted and measured fiber length distributions for Location B on the slow-fill 30wt% LCF/PA66 plaque.

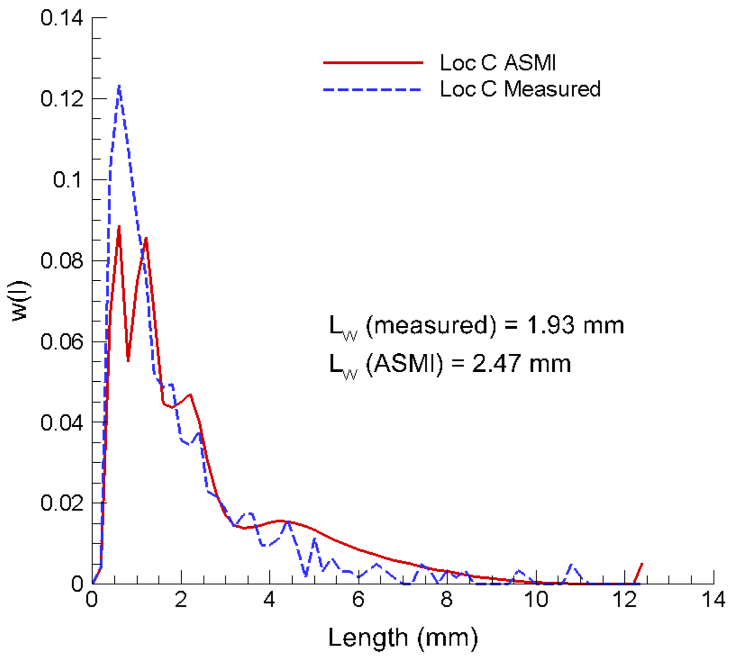

Figure 19. Predicted and measured fiber length distributions for Location C on the slow-fill 30wt% LCF/PA66 plaque.

Tensile Modulus	E_{11} (predicted FLD) MPa	E_{11} (measured FLD) MPa	**Agreement within**
Loc. A	22499	22309	0.85%
Loc. B	25500	25427	0.29%
Loc. C	26310	26106	0.78%

Table 17. Computed E_{11} based on measured and predicted fiber length distributions at Locations A, B and C in the slow-fill 30wt% LCF/PA66 edge-gated plaque.

Tensile Modulus	E_{22} (predicted FLD) MPa	E_{22} (measured FLD) MPa	Agreement within
Loc. A	24620	24408	0.87%
Loc. B	19802	19749	0.27%
Loc. C	19123	18987	0.72%

Table 14. Computed E_{22} based on measured and predicted fiber length distributions at Locations A, B and C in the slow-fill 30% LCF/PA66 edge-gated plaque.

Flexural Modulus	D_{11} (predicted FLD) $MPa.mm^3$	D_{11} (measured FLD) $MPa.mm^3$	Agreement within
Loc. A	86813	86085	0.85%
Loc. B	86750	86511	0.28%
Loc. C	88210	87556	0.75%

Table 15. Computed D_{11} based on measured and predicted fiber length distributions at Locations A, B and C in the slow-fill 30wt% LCF/PA66 edge-gated plaque.

Flexural Modulus	D_{22} (predicted FLD) $MPa.mm^3$	D_{22} (measured FLD) $MPa.mm^3$	Agreement within
Loc. A	56729	56320	0.73%
Loc. B	53404	53282	0.23%
Loc. C	51807	51493	0.61%

Table 16. Computed D_{22} based on measured and predicted fiber length distributions at Locations A, B and C in the slow-fill 30wt% LCF/PA66 edge-gated plaque.

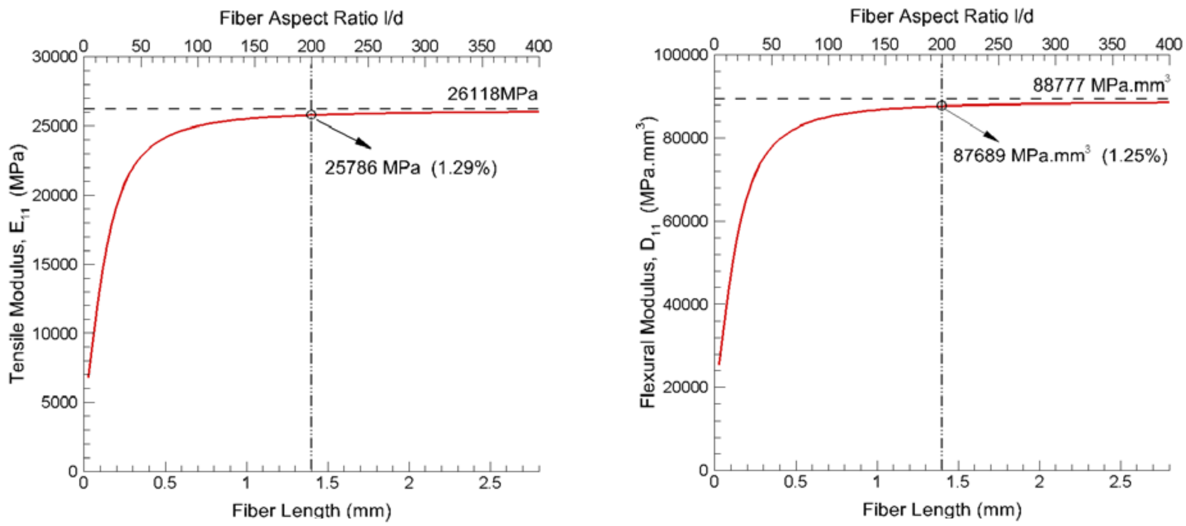

(a) (b)

Figure 20. Sensitivity analysis of fiber length showing saturation of elastic moduli in the range of long fibers for the 30wt% LCF/PA66 molding – (a) E_{11} and (b) D_{11}.

4.3 Implementation and Improvements of Process Models in ASMI (Autodesk)

Autodesk delivered a new research version of ASMI to PNNL. The new research version includes the improved 3D fiber orientation solver. The inlet orientation condition strongly influences the orientation predicted in the part by the RSC model. The option to specify the inlet profile, which was already available in the ASMI Miplane and Dual Domain solver, has been added in the 3D solver. A new option was added in the new research version of ASMI to apply the prescribed inlet orientation profile through the thickness direction of the part around the gate. The dialog boxes including the new options are shown in Figure 21. The previous section on *3D fiber orientation modeling* in this report demonstrated significant improvements in 3D fiber orientation predictions using this new ASMI version (Figures 6 to 11). In the 3D analyses of the slow-fill 50wt% LCF/PP edge-gated and center-gated plaques, we prescribed the same inlet condition and the same ARD-RSC model parameters as used in the corresponding midplane models. The predictions by the ARD-RSC model exhibit good agreement with fiber orientation data.

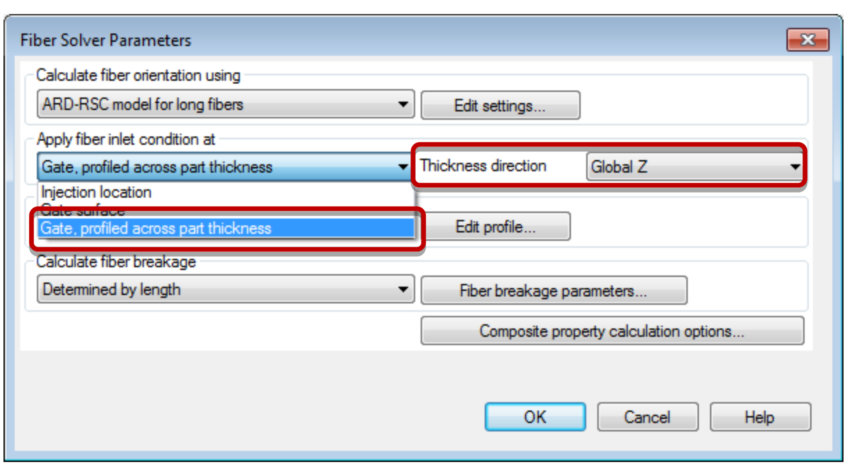

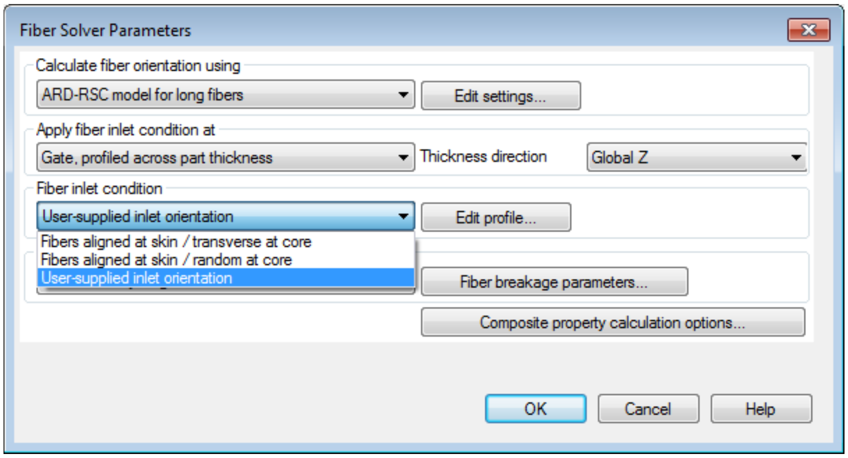

Figure 21. New options in the research version of ASMI for 3D fiber orientation prediction.

4 Publications/Presentations

Jin Wang, Ba Nghiep Nguyen, Raj Mathur, Bhisham Sharma, Michael D Sangid, Franco Costa, Xiaoshi Jin, Charles L. Tucker III and Leonard S. Fifield. "FIBER ORIENTATION IN INJECTION MOLDED LONG CARBON FIBER THERMOPLASTIC COMPOSITES", Society of Plastic Engineers, Annual Technical Conference (SPE-ANTEC), Orlando, March 23-25, 2015.

5 Patents

None

6 Future Plans

PNNL continues to run 3D ASMI analyses for all the PlastiComp plaques on the go/no-go list. Autodesk will complete 3D fiber orientation model improvement and will deliver to PNNL a new research version of ASMI for completing ASMI analyses of PlastiComp plaques. Magna will kick off the tooling for the complex 3D part and PlastiComp will produce carbon fiber-filled materials to be used for part molding.

7 Budgetary Information

	Budget Period 1									
	FY13-Q1		FY13-Q2		FY14-Q1		FY14-Q2		FY14-Q3	
Baseline Reporting Quarter	9/11/2012 - 12/31/2012		1/1/2013 - 3/31/2013		10/1/2013 - 12/31/2013		1/1/2014 - 3/31/2014		4/1/2014 - 6/30/2014	
	Q1	Cumulative Total	Q2	Cumulative Total	Q1	Cumulative Total	Q2	Cumulative Total	Q3	Cumulative Total
Baseline Cost Plan										
Federal Share	$6,808	$6,808	$2,536	$9,344	$62,859	$73,365	$117,143	$190,508	$87,207	$277,715
Non-Federal Share	$0	$0	$0	$0	$178,823	$178,823	$219,222	$398,045	$160,040	$558,085
Total Planned	$6,808	$6,808	$2,536	$9,344	$241,682	$252,188	$336,365	$588,553	$247,247	$835,800
Actual Incurred Cost										
Federal Share	$6,808	$6,808	$2,536	$9,344	$62,859	$73,365	$117,143	$190,508	$87,207	$277,715
Non-Federal Share	$0	$0	$0	$0	$172,553	$172,553	$219,222	$391,774	$160,040	$551,814
Total Incurred Costs	$6,808	$6,808	$2,536	$9,344	$235,412	$245,917	$336,365	$582,282	$247,247	$829,529
Variance										
Federal Share	$0	$0	$0	$0	$0	$0	$0	$0	$0	$0
Non-Federal Share	$0	$0	$0	$0	$6,270	$6,270	$0	$6,271	$0	$6,271
Total Variance	$0	$0	$0	$0	$6,270	$6,270	$0	$6,271	$0	$6,271

	FY14-Q4		FY15-Q1		FY15-Q2	
Baseline Reporting Quarter	7/1/2014 - 9/30/2014		10/1/2014 - 12/31/2014		1/1/2015 - 3/31/2015	
	Q4	Cumulative Total	Q1	Cumulative Total	Q2	Cumulative Total
Baseline Cost Plan						
Federal Share	$90,514	$368,229	$123,156	$491,385	$101,927	$593,312
Non-Federal Share	$12,269	$570,354	$0	$570,354	$102,294	$672,648
Total Planned	$102,783	$938,583	$123,156	$1,061,739	$204,221	$1,265,960
Actual Incurred Cost						
Federal Share	$90,514	$368,229	$149,162	$517,391	$71,374	$588,765
Non-Federal Share	$223,162	$774,976	$180,636	$955,613	$127,783	$1,083,395
Total Incurred Costs	$313,676	$1,143,205	$329,798	$1,473,003	$199,157	$1,672,160
Variance						
Federal Share	$0	$0	-$26,006	-$26,006	$30,553	$4,547
Non-Federal Share	-$210,893	-$204,622	-$180,636	-$385,259	-$25,489	-$410,748
Total Variance	-$210,893	-$204,622	-$206,642	-$411,264	$5,064	-$406,201

	Budget Period 2							
	FY15-Q3		FY15-Q4		FY16-Q1		FY16-Q2	
Baseline Reporting Quarter	4/1/2015 - 6/30/2015		7/1/2015 - 9/30/2015		10/1/2015 - 12/31/2015		1/1/2016 - 3/31/2016	
	Q3	Cumulative Total	Q4	Cumulative Total	Q1	Cumulative Total	Q2	Cumulative Total
Baseline Cost Plan								
Federal Share	$101,927	$695,239	$101,927	$797,166	$101,927	$899,094	$101,927	$1,001,021
Non-Federal Share	$102,294	$774,941	$102,294	$877,235	$102,294	$979,528	$102,294	$1,081,822
Total Planned	$204,221	$1,470,181	$204,221	$1,674,401	$204,221	$1,878,622	$204,221	$2,082,843
Actual Incurred Cost								
Federal Share		$588,765		$588,765		$588,765		$588,765
Non-Federal Share		$1,083,395		$1,083,395		$1,083,395		$1,083,395
Total Incurred Costs	$0	$1,672,160	$0	$1,672,160	$0	$1,672,160	$0	$1,672,160
Variance								
Federal Share								
Non-Federal Share								
Total Variance								

8 References

[1] Phelps JH and Tucker III CL (2009). An Anisotropic Rotary Diffusion Model for Fiber Orientation in Short- and Long-Fiber Thermoplastics, Journal of the Non-Newtonian Fluid Mechanics, 156(3):165-176.

[2] Nguyen BN, Fifield LS, Kijewski SA, Sangid MD, Wang J, Jin X, Costa F, Tucker III CL, Mathur RN, Gandhi UN, and Mori S (2015). “Predictive Engineering Tools for Injection-molded Long-Carbon Fiber Thermoplastic Composites,” Quarterly Report, PNNL-24031.

[3] Phelps JH, Abd El-Rahman AI, Kunc V, and Tucker III CL 2013. “A Model for Fiber Length Attrition in Injection-molded Long-fiber Composites,” Composites: Part A, 51, 11-21.

[4] Tucker III CL (2012). “Improved Fiber Length Model for Injection-Molded LFT Composites,” Progress Report to The American Chemistry Council, University of Illinois at Urbana-Champaign, Urbana, IL.

Pacific Northwest
NATIONAL LABORATORY

U.S. DEPARTMENT OF
ENERGY

Proudly Operated by Battelle *Since 1965*

902 Battelle Boulevard
P.O. Box 999
Richland, WA 99352
1-888-375-PNNL (7665)

www.pnnl.gov